Generation and validation of a PITX2–EGFP reporter line of human induced pluripotent stem cells enables isolation of periocular mesenchymal cells

Received for publication, August 22, 2019, and in revised form, February 5, 2020 Published, Papers in Press, February 7, 2020, DOI 10.1074/jbc.RA119.010713

Toru Okubo[‡§], Ryuhei Hayashi[‡¶1], Shun Shibata[‡§], Yuji Kudo[‡§], Yuki Ishikawa[¶], Saki Inoue[¶], Yuki Kobayashi[¶], Ai Honda[¶], Yoichi Honma[‡§], Satoshi Kawasaki[¶], and Kohji Nishida[¶‖]

From the Departments of [‡]Stem Cells and Applied Medicine and [¶]Ophthalmology, Graduate School of Medicine and the [‖]Integrated Frontier Research for Medical Science Division, Institute for Open and Transdisciplinary Research Initiatives, Osaka University, Suita, Osaka 565-0871, Japan and the [§]Basic Research Development Division, Rohto Pharmaceutical Co., Ltd., Osaka 544-8666, Japan

Edited by Xiao-Fan Wang

PITX2 (Paired-like homeodomain transcription factor 2) plays important roles in asymmetric development of the internal organs and symmetric development of eye tissues. During eye development, cranial neural crest cells migrate from the neural tube and form the periocular mesenchyme (POM). POM cells differentiate into several ocular cell types, such as corneal endothelial cells, keratocytes, and some ocular mesenchymal cells. In this study, we used transcription activator–like effector nuclease technology to establish a human induced pluripotent stem cell (hiPSC) line expressing a fluorescent reporter gene from the *PITX2* promoter. Using homologous recombination, we heterozygously inserted a PITX2–IRES2–EGFP sequence downstream of the stop codon in exon 8 of *PITX2*. Cellular pluripotency was monitored with alkaline phosphatase and immunofluorescence staining of pluripotency markers, and the hiPSC line formed normal self-formed ectodermal autonomous multizones. Using a combination of previously reported methods, we induced PITX2 in the hiPSC line and observed simultaneous EGFP and PITX2 expression, as indicated by immunoblotting and immunofluorescence staining. *PITX2* mRNA levels were increased in EGFP-positive cells, which were collected by cell sorting, and marker gene expression analysis of EGFP-positive cells induced in self-formed ectodermal autonomous multizones revealed that they were genuine POM cells. Moreover, after 2 days of culture, EGFP-positive cells expressed the PITX2 protein, which co-localized with forkhead box C1 (FOXC1) protein in the nucleus. We anticipate that the PITX2–EGFP hiPSC reporter cell line established and validated here can be utilized to isolate POM cells and to analyze PITX2 expression during POM cell induction.

Neural crest cells (NCCs)[2] are multipotent stem cells generated at the border between the neural tube and surface ectoderm during early embryonic development in vertebrates (1). In eye development, cranial NCCs migrate to form the periocular mesenchyme (POM). POM cells in turn differentiate into a wide variety of cells, such as corneal endothelial cells (2), keratocytes, iris stromal cells, ciliary muscle cells, trabecular meshwork cells, and scleral cells (3, 4). In addition, peripheral tissues of the eyes, such as cartilage, bone, dermis, and fat, which are connected to the extraocular muscles, also originate from POM cells (5).

PITX2 (paired-like homeodomain transcription factor 2) is one of the homeobox transcription factors that play key roles during embryogenesis. PITX2 is crucial in left–right asymmetry in visceral organs (6), such as the heart (7–9), lungs (7), gut (8, 10), and stomach, as well as in eye development (11). In the eyes, PITX2 is expressed in the cranial NC-derived POM cells, together with other transcription factors, such as FOXC1, FOXC2 (12), and LMX1B (13), and plays important roles in ocular anterior segment development (14). Specifically, PITX2 is involved in the development of corneal endothelial cells (15), keratocytes (16), iris stromal cells (17), ciliary muscles, trabecular meshwork cells, scleral cells, mesenchymal cells of the ocular glands, and peripheral connective tissues connected to the extraocular muscles (18). Mutation of PITX2 or FOXC1 causes Axenfeld–Rieger syndrome, which manifests with dysgenesis of the anterior segment of the eyes as well as mild tooth malformation and craniofacial dysmorphism (19, 20).

It has been suggested that POM cells can be induced from human induced pluripotent stem cells (hiPSCs) (21). We recently reported that hiPSCs form self-formed ectodermal autonomous multizones (SEAMs) from which ocular cells, such as corneal epithelial cells, conjunctival epithelial cells, lens cells, retinal cells, and NCCs, can be derived (22, 23). In SEAMs,

This work was supported in part by the Project for the Realization of Regenerative Medicine of the Japan Agency for Medical Research and Development. R. H. is affiliated with the endowed chair of Rohto Pharmaceutical Co., Ltd. T. O., S. S., Y. Kudo, and Y. H. are employees of Rohto Pharmaceutical Co., Ltd.

This article contains Figs. S1–S3.

[1] To whom correspondence should be addressed: Dept. of Stem Cells and Applied Medicine, Osaka University Graduate School of Medicine, Suita, Japan, 2-2 Yamadaoka, Suita, Osaka 565-0871, Japan. Tel.: 81-6-6210-8387; Fax: 81-6-6210-8388; E-mail: ryuhei.hayashi@ophthal.med.osaka-u.ac.jp.

[2] The abbreviations used are: NCC, neural crest cell; POM, periocular mesenchyme; hiPSC, human induced pluripotent stem cell; SEAM, self-formed ectodermal autonomous multizone; TALEN, transcription activator–like effector nuclease; E*n*, embryonic day *n*; MEF, mouse embryonic fibroblast; ALP, alkaline phosphatase; qRT-PCR, quantitative RT-PCR; DM, differentiation medium; EGF, epidermal growth factor; bFGF, basic fibroblast growth factor; PE, phycoerythrin.

various types of cells mimic their differentiation process to form a whole eye structure *in vitro*. We expect that SEAMs contain PITX2-expressing POM cells differentiated from NCCs. However, it is nearly impossible to isolate PITX2-expressing POM cells from the various cell types in culture systems without a reporter line, because POM cell-specific cell-surface markers have not been reported to date.

Transcription activator–like effector nucleases (TALENs) are restriction enzymes that generate site-specific double-strand breaks in DNA, with lower nonspecific cleavage activity (24) than CRISPR-Cas (25), through binding of a TAL effector to specific DNA regions (26). The double-strand breaks are repaired through nonhomologous end joining or homologous recombination. TALENs can be used for specific gene knockout or knockin. We previously demonstrated that a p63 knockin reporter line generated with TALEN technology could be used for detailed analysis and isolation of p63-positive cells in SEAMs (27).

Here, we report the generation of a PITX2 reporter line of hiPSCs harboring an IRES2-EGFP sequence, using TALEN technology. We validated the reporter line in a system in which PITX2 expression is induced in pluripotent stem cells. In addition, we were able to isolate and analyze POM cells. The PITX2 reporter hiPSC line generated in this study allows robust induction and isolation of POM-derived cells and insights into the detailed mechanisms of induction of POM cells and POM cell-derived cells.

Results

PITX2 is expressed in POM cells in the mouse embryo

We evaluated Pitx2 expression in POM cells in mouse embryos at E10.5 (Fig. S1*A*) and E12.5 (Fig. S1*B*). At both stages, cells ranging from the periocular sites to primordial cells of the cornea were positive for Pitx2 and Foxc1, but negative for Sox10, a negative marker of POM cells. This finding indicated that POM cells exist in the periocular sites in E10.5 and E12.5 mouse embryos.

Evaluation of GFP fluorescence intensity driven by the PITX2 promoter

To achieve strong GFP fluorescence upon forced expression in 293T cells, various GFP variants, polycistronic sequences, and polyadenylation (poly(A)) signals were evaluated. First, three GFPs—EGFP, EmGFP, and TurboGFP—were inserted downstream of the *PITX2* and 2A peptide sequences in pEF5/FRT/V5-DEST. There were no obvious differences in intensity between these three GFPs (Fig. S2*A*). As polycistronic sequences, 2A peptides and IRES2 were evaluated. Fluorescence intensity was stronger when *EGFP* was located downstream of IRES2 than when it was downstream of the 2A peptide sequences (Fig. S2*B*). As for polyadenylation, poly(A) signals of bovine growth hormone, herpes simplex virus–thymidine kinase, SV40, PITX2 3′-UTR, and β-actin 3′-UTR were evaluated. SV40 and PITX2 3′-UTR yielded slightly stronger EGFP intensity than the other poly(A) signals (Fig. S2*C*). Based on our findings, we used a donor vector containing EGFP, IRES2, and SV40 as the GFP variant, polycistronic sequence, and polyadenylation signal, respectively, for establishing a PITX2–GFP reporter hiPSC line.

Design of a TAL effector and donor vector

There are six splice variants of *PITX2* and three isoforms (Fig. 1*A*). Exon 8 is common to all *PITX2* variants. Thus, we added the artificial sequences downstream of *PITX2* exon 8. As shown in Fig. 1*B*, a TAL effector recognition site in the left arm was located immediately upstream of a stop codon of *PITX2*, and a right-arm recognition site was designed after the *PITX2* stop codon. The donor vector was designed so that IRES2–EGFP–SV40 poly(A) followed the left arm of *PITX2* with a silent mutation to avoid the generation of double-strand breaks after successful site-specific double-strand break generation by the TALEN.

Generation of a PITX2–EGFP knockin reporter hiPSC line

After electroporation of the TALEN vector and donor vector into 201B7 hiPSCs, the cells were seeded on DR4 mouse embryonic fibroblasts (MEFs) for drug selection. Knockin cells were screened on G418 sulfate as outlined in Fig. 2*A*. Based on PCR results, colony 8 (IRES2) was selected for further recloning analysis (Fig. 2*B*). Colonies 5 and 7 (2A) seemed to be successfully transfected; however, they were not further analyzed because the 2A peptides yielded lower EGFP intensity as shown in Fig. S2*B*. Colony 8 was recloned, and six colonies were analyzed by PCR, which revealed that the construct was heterozygously introduced in all six colonies. Colony 8-2 produced a slightly stronger band intensity than the other colonies (Fig. 2*C*) and was therefore chosen as the best candidate PITX2–EGFP hiPSC reporter line for further analysis. The genome sequence of this line was confirmed using Sanger sequencing (Fig. S3).

Pluripotent stem cell markers and typical SEAM phenotypes in the PITX2–EGFP knockin reporter line

After passaging the PITX2 knockin hiPSC line for feeder-free culture, the cells formed round, normal colonies on iMatrix-511, as shown in Fig. 3*A*. In an alkaline phosphatase (ALP)–staining assay, PITX2 knockin hiPSC clone 8-2 showed a staining intensity and color similar to those of 201B7 WT hiPSCs (Fig. 3*B*). Expression of the pluripotent markers NANOG, OCT3/4, TRA-1–60, and SSEA-4 was evaluated by immunofluorescence analysis using specific antibodies. All these markers showed strong expression from the center to the borders of the colonies (Fig. 3*C*). We successfully induced SEAM structures consisting of four zones using the PITX2 knockin hiPSC line as reported previously (22, 23). After SEAM induction, markers of corneal epithelial cells (p63, PAX6) lens cells (p63, α-crystallin), neuroretina (CHX10), and retinal pigment epithelial cells (MITF) were stained (Fig. 3*D*). The cells in zone 3 were p63- and PAX6-positive and showed cobblestone morphology, which indicated that they were corneal epithelial cells. The aggregated cells at the end of zone 2 were p63- and α-crystallin–positive lens cells. The cells in the inner area of zone 2 were CHX10-positive neuroretinal cells. The cells aggregated in the outer area of zone 2 were MITF-positive retinal pigment epithelial cells. All these structures were similar to those induced in 201B7 hiPSCs. We also evaluated gene expression patterns in SEAMs (Fig. 3*E*). Expression of *TUBB3*, a neuron marker, was substantially higher in zone 1. Expression of the neural crest cell marker *SOX10* and the neural retina marker *RAX* was higher in zone 2. *PAX6* was expressed in all

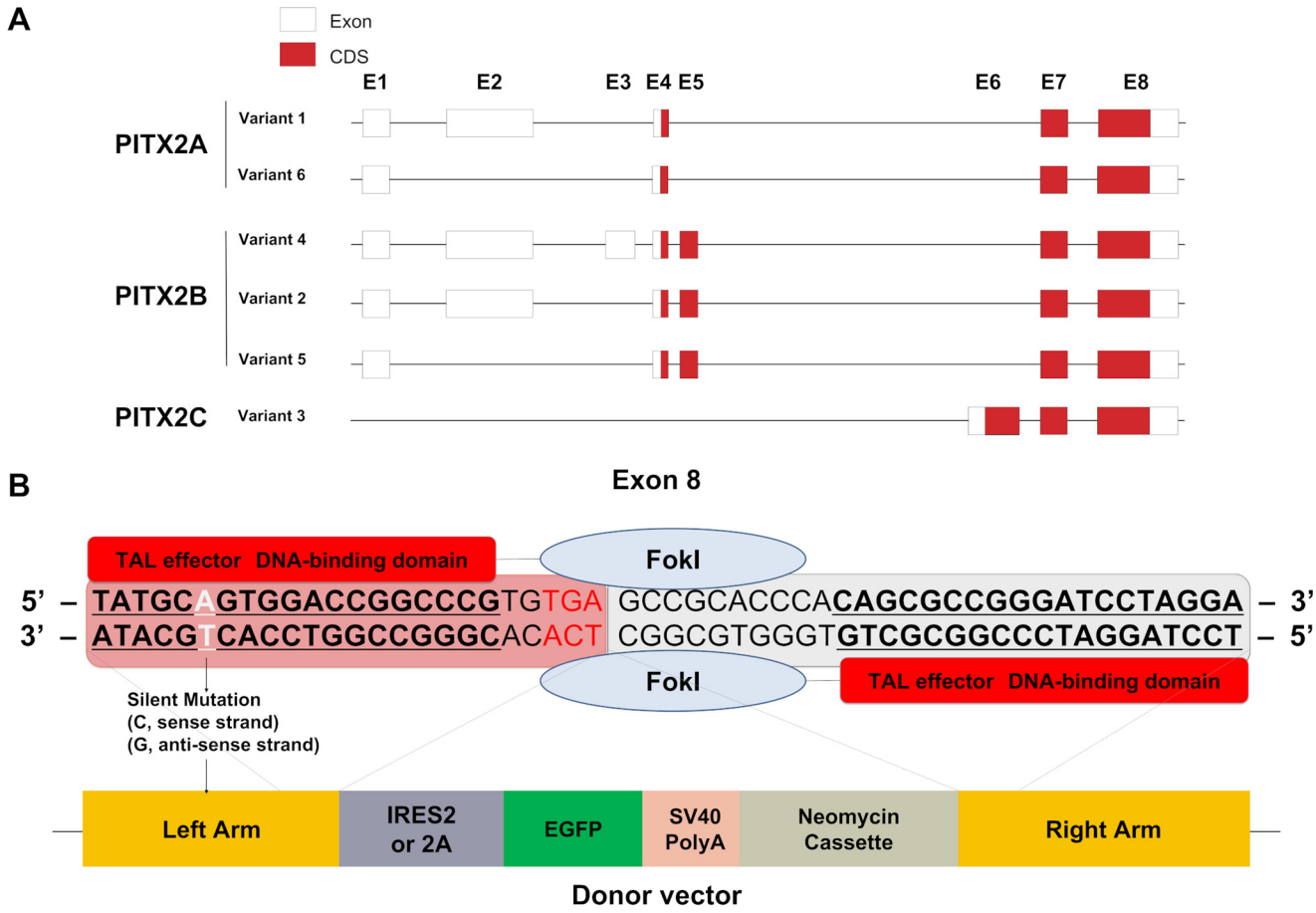

Figure 1. Schematic diagram of splice variants of *PITX2* and structure of the donor vector used for gene knockin. *A*, splice variants and isoforms of PITX2. *White* and *red boxes* indicate untranslated and coding sequences, respectively. Exons are *numbered*. *B*, structure of the donor vector used for establishing the *PITX2*-based reporter systems. The TAL effector DNA-binding domain (*underline*) and the location of a silent mutation (*C*, sense strand; *G*, antisense strand) are indicated. *PITX2*, paired-like homeodomain transcription factor 2; *CDS*, coding sequence; *E*, exon; *TAL*, transcription activator–like.

zones. Epithelial markers *DN-p63*, *CDH1*, and *KRT18* were highly expressed in zones 3 and 4. The lens cell marker *CRYAA* was the most strongly expressed in zones 3 and 4. This expression pattern was similar to that of 201B7 hiPSCs (22).

Validation of the PITX2–EGFP knockin reporter line

To confirm that EGFP is expressed in the PITX2 knockin hiPSC line, POM cells were induced by a combination of reported induction methods (28–31) (Fig. 4*A*). Aggregated cells were detected ~20 days after the start of induction (Fig. 4*B*). The aggregated cells showed EGFP signals at day 20 (Fig. 4*C*). We determined EGFP and PITX2 protein expression levels using whole cell lysates by Western blotting analyses. PITX2 expression in knockin iPSCs was nearly the same as that in clone 8-2 PITX2 knockin iPSCs (Fig. 4*D*), and we observed robust protein expression of EGFP in PITX2 knockin iPSC clone 8-2. Next, we conducted immunofluorescence staining using anti-PITX2 antibody to evaluate whether EGFP and PITX2 are expressed simultaneously. As shown in Fig. 4*E*, EGFP fluorescence and PITX2 fluorescent staining were detected simultaneously. Next, we sorted and collected EGFP-positive and -negative cells by FACS (Fig. 4*F*). We analyzed PITX2 expression levels by quantitative RT-PCR (qRT-PCR). The population of EGFP-positive cells exhibited high *PITX2* expression, whereas EGFP-negative cells hardly expressed *PITX2*. Moreover, *FOXC1* and *TFAP2B*, which are markers of POM cells, were significantly more strongly expressed in EGFP-positive cells when compared with EGFP-negative cells. Conversely, *SOX10*, which is a negative marker of POM cells, was more strongly expressed in EGFP-negative than in EGFP-positive cells. On the other hand, the POM markers *FOXC2*, *LMX1B*, *NGFR*, *LMX1B*, and *COL8A2* were not highly expressed in EGFP-positive cells (Fig. 4*G*).

Isolation and characterization of POM cells

To acquire more genuine POM cells, we tried a SEAM induction method (Fig. 5*A*). Typical, aggregated cells emerged in SEAM zone 2 after 14 days of induction (Fig. 5*B*). EGFP signals were confirmed at the location of aggregated cells in SEAM zone 2 (Fig. 5*C*). After sorting EGFP-positive cells (Fig. 5*D*), they were analyzed for marker expression by qRT-PCR. All positive POM cell markers were significantly increased in EGFP-positive compared with EGFP-negative cells, and there was no difference of *SOX10* expression level between them (Fig. 5*E*), which revealed that the EGFP-positive cells were POM cells. They were cultivated for 2 days in a culture plate using differentiation medium (DM) with Y-27632, epidermal growth factor (EGF), basic fibroblast growth factor (bFGF), and retinoic acid (Fig. 5*F*). Cells expressed PITX2 protein, which co-localized with FOXC1 protein in the nucleus (Fig. 5*G*).

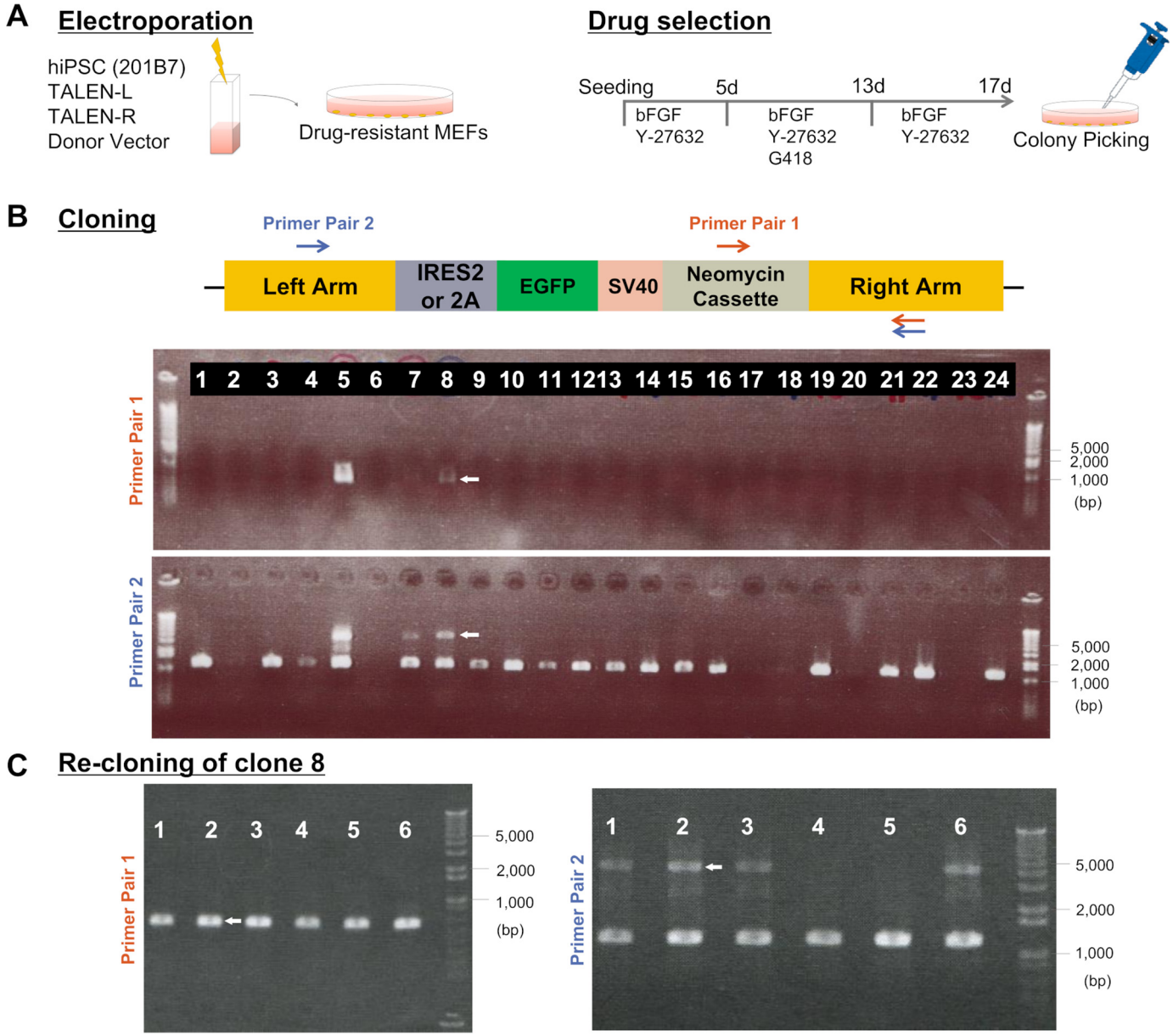

Figure 2. Protocol for PITX2–EGFP knockin and cloning. *A*, schematic representation of the protocols for electroporation of TALEN plasmid and PITX2 reporter donor vector into 201B7 hiPSCs grown on drug-resistant MEFs and drug selection. *B*, PCR analysis of PITX2–EGFP knockin reporter line candidate clones. *Odd numbers* indicate samples for which 2A peptides were used, and *even numbers* indicate samples for which IRES2 was used as a polycistronic sequence. Binding sites for primer pairs 1 and 2 are indicated as *red* and *blue arrows*, respectively. The amplicon size of primer pair 1 is 598 bp for knockin, whereas amplicon sizes of primer pair 2 are 3677 (3150 when 2A is used) and 1191 bp for knockin and WT, respectively. *Arrows* indicate the amplicons that prove successful knockin in the candidate clones. *C*, PCR analysis upon recloning of clone candidate 8. *Arrows* (clone 8-2) indicate the amplicons that prove successful knockin in the candidate clones of recloning.

Discussion

Various GFP variants, polycistronic sequences, and poly(A) signals were evaluated in a stepwise manner to establish a PITX2–EGFP knockin hiPSC reporter line with optimum GFP expression. The GFP variants EGFP, EmGFP, and TurboGFP did not show a difference in fluorescence intensity. Unexpectedly, the IRES2 sequence yielded stronger EGFP fluorescence than the 2A peptides. The 2A peptides were added at the C terminus of *PITX2*, and the proline added at the N terminus of GFP might have affected GFP expression or fluorescence. Alternatively, unknown mechanisms might determine the compatibility between target gene and following polycistronic sequences. The various polyadenylation signals tested yielded slightly different EGFP expression. Interestingly, among them, poly(A) of SV40 and PITX2 3′-UTR had the strongest ability to stabilize *PITX2* mRNA.

The efficiency of PITX2–IRES2–EGFP knockin was 1 of 12. This was more or less as expected, but there is room for improving the knockin efficiency, for example by increasing the vector concentrations and optimizing the electroporation program.

The reporter line established in this study showed normal pluripotency based on ALP staining and immunofluorescence staining of the markers analyzed in this study. We confirmed that a PITX2 knockin hiPSC line formed typical SEAMs and

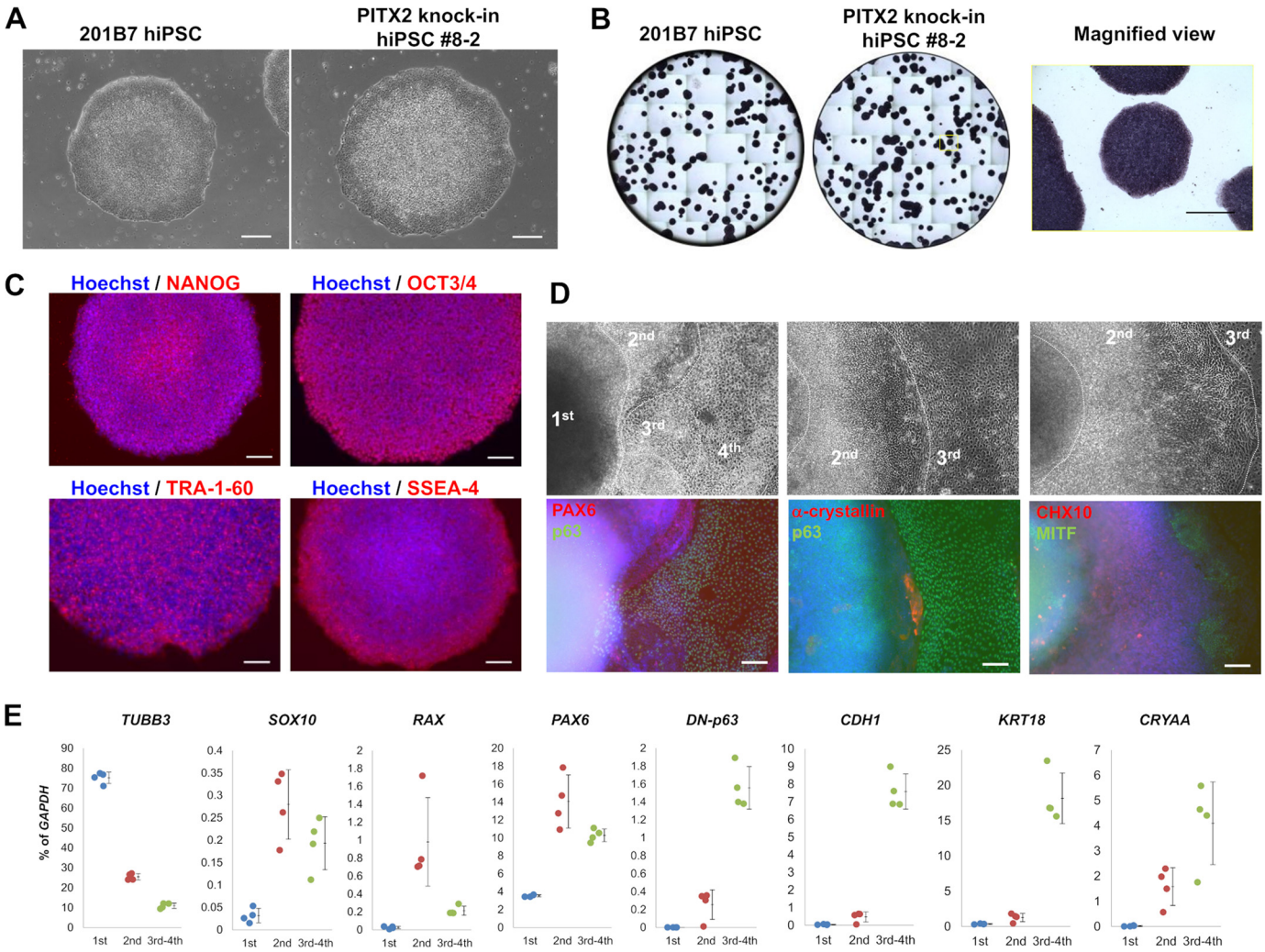

Figure 3. Confirmation of pluripotency of PITX2–EGFP knockin hiPSC clone 8-2. *A*, phase-contrast image of 201B7 hiPSCs and PITX2 knockin hiPSC clone 8-2. *Scale bars*, 200 μm. *B*, ALP staining of 201B7 hiPSCs and PITX2 knockin hiPSC clone 8-2. The *left panels* are macro images of staining, and the *right panel* shows magnifications of the *yellow* indicated areas. *Scale bars*, 1000 μm in the *left panel* and 400 μm in the *right panel*. *C*, immunofluorescence staining of pluripotent markers, NANOG, OCT3/4, TRA-1–60, and SSEA-4 in PITX2 knockin hiPSC clone 8-2 cells. *Scale bars*, 50 μm. *D*, immunofluorescence staining of SEAMs after 5 weeks for corneal epithelial cells (p63/PAX6), 8 weeks for lens cells (p63/a-crystallin), and 5 weeks for neuroretinal cells (CHX10), and retinal pigment epithelial cell (MITF). *Scale bars*, 100 μm. *E*, gene expression patterns in cells that were manually harvested from each SEAM zone induced from PITX2–EGFP knockin hiPSC clone 8-2. Expression levels are presented as dot plots of each value and the means ± standard deviation ($n = 4$).

showed a robust ability to induce lens cells, neuroretinal cells, and retinal pigment cells, although they induced less corneal epithelial cells than 201B7 hiPSCs did (Fig. 3*D*). Such a difference in differentiation tendency often occurs among pluripotent stem cell lines (32).

We were able to establish PITX2-expressing cells by combining published approaches: NC induction by WNT and low BMP signaling (28), corneal endothelial cell induction by EGF treatment, and FGF signaling for POM cell-derived tissue induction (29). Unfortunately, the cells did not show perfect gene expression patterns of POM cells, although they showed high *FOXC1* mRNA expression and low *SOX10* mRNA expression, which are characteristic for POM cells (12, 33). However, PITX2-expressing cells induced by the SEAM method did show perfect gene expression patterns of POM cells based on qRT-PCR results (Fig. 5*E*). Moreover, *COL8A2* and *COL8A1*, which are markers of POM and corneal endothelial cell, were significantly increased in EGFP-positive cells. This might indicate that they are POM cells and have a potential to differentiate into POM-derived cells. In the near future, we would like to utilize this cell line to further analyze POM cells in SEAM-inducing and other culture conditions.

In conclusion, we successfully generated and validated a PITX2–IRES2–EGFP knockin hiPSC line, and we were able to isolate PITX2-expressing POM cells. These cells showed higher POM marker expression than EGFP-negative cells. The POM cells sorted in this study are a reliable tool for detailed analysis of POM-derived ocular cells. Our reporter line provides a technical platform for testing induction methods and for detailed analysis of PITX2-expressing cells and their derivatives.

Experimental procedures

Immunostaining of mouse embryos

All animal experimental protocols in this study were in accordance with the Association for Research in Vision and

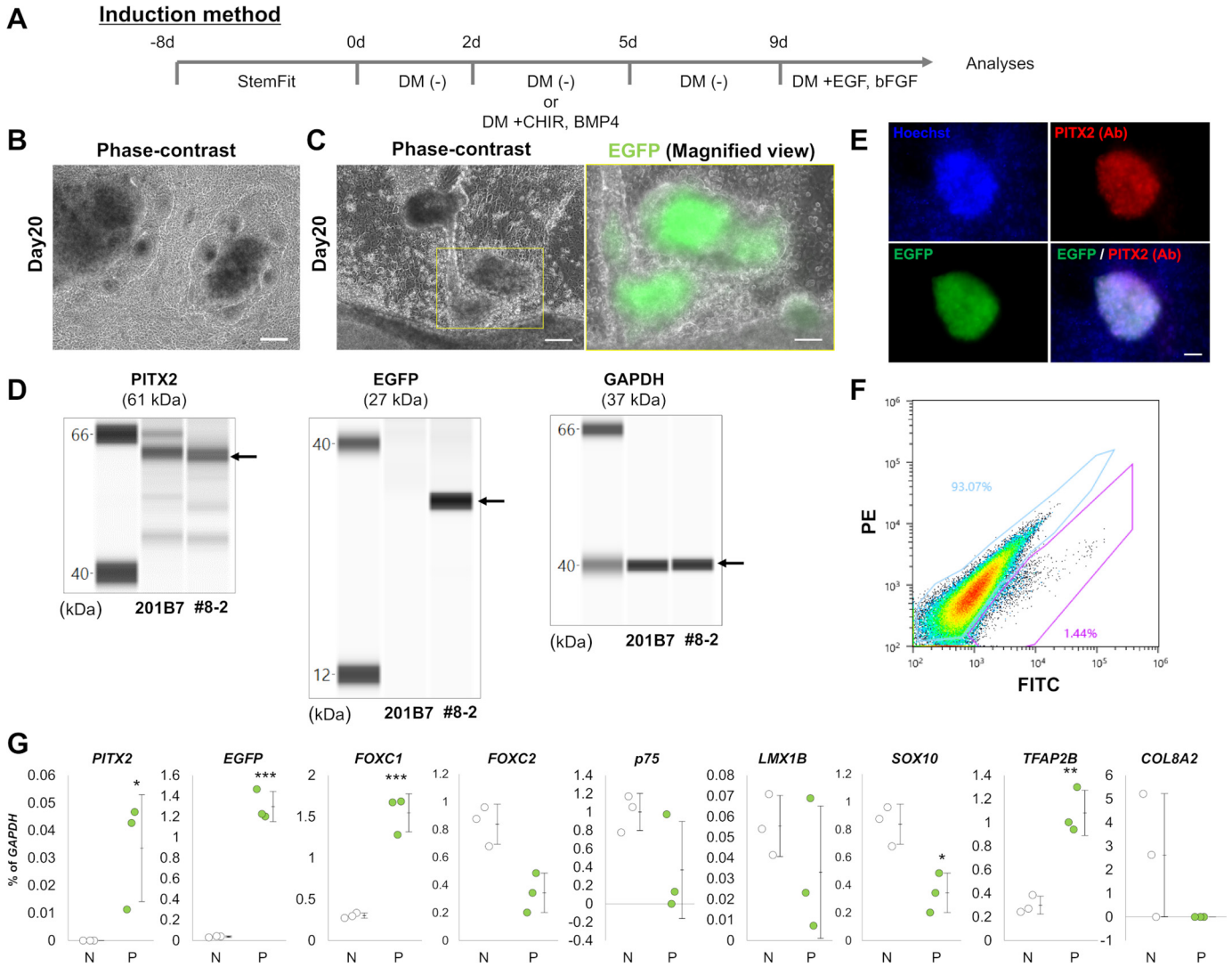

Figure 4. Correlation between PITX2 and EGFP expression in PITX2–EGFP knockin hiPSC clone 8-2 cells. *A*, schematic representation of the protocol used for PITX2 induction. *B*, phase-contrast images of PITX2 knockin hiPSC clone 8-2. *Scale bar*, 200 μm. *C*, phase-contrast and fluorescence images of aggregated PITX2 knockin hiPSC clone 8-2 that express EGFP fluorescence. *Scale bar*, 100 μm in the *left panel* and 50 μm in the *right panel*. *D*, Western blotting analysis of PITX2 (61 kDa), EGFP (27 kDa), and GAPDH (37 kDa) in PITX2 knockin hiPSC clone 8-2. *E*, image of immunofluorescence staining of PITX2 knockin hiPSC clone 8-2 cells that express PITX2 (*red*) and EGFP fluorescence (*green*). *Scale bar*, 50 μm. *F*, FACS analysis of EGFP fluorescence intensity in 201B7 hiPSCs and PITX2 knockin hiPSC clone 8-2. The cells were expanded in PE (*y* axis) and FITC (*x* axis). The cells were selected using polygon gates; cells in the *blue polygon* are EGFP-negative, and those in the *purple polygon* are EGFP-positive. *G*, mRNA expressions of positive and negative markers of POM cell as determined by qRT-PCR in EGFP-negative and -positive cells after cell sorting. Expression levels are presented as dot plots of each value and the means ± standard deviation ($n = 3$). *, $p < 0.05$; **, $p < 0.01$; ***, $p < 0.001$. *N*, negative cells; *P*, positive cells.

Ophthalmology Statement for the Use of Animals in Ophthalmic and Visual Research, with prior approval from the Animal Ethics Committee of Osaka University. E10.5 and E12.5 ICR mice were purchased from Japan SLC (Sizuoka, Japan). After the mice were euthanized with pentobarbital sodium, they were perfused with PBS. Mouse embryos were collected and were also euthanized. They were embedded in Tissue-Tek O.C.T. compound (Sakura Finetek Japan, Tokyo, Japan), frozen on dry ice, and stored at −80 °C. The mouse embryos were sectioned and incubated with blocking solution (5% normal donkey serum, 0.3% Triton X-100 in TBS). Then the sections were incubated with primary antibodies against PITX2 (Ab55599; Abcam, Cambridge, MA), FOXC1 (8758S; Cell Signaling Technology), and SOX10 (sc-17342; Santa Cruz Biotechnology) at 4 °C overnight, followed by secondary antibodies conjugated with Alexa Flour 488, Alexa Flour 568, Alexa Flour 594, and Alexa Flour 647 (Thermo Fisher Scientific) for 1 h. The sections were counterstained with Hoechst 33342 (Thermo Fisher Scientific) and visualized and imaged under an Axio Observer D1 microscope (Carl Zeiss).

Analysis of fluorescence intensity

293T cells were seeded in a 6-well plate at $3.0–4.0 \times 10^5$ cells/well. Constructs for forced expression in 293T cells were synthesized using Gateway LR Clonase II (Thermo Fisher Scientific) and the pEF5/FRT/V5-DEST vector (Thermo Fisher Scientific). FuGENE HD transfection reagent (Promega, Madison, WI) and 1.3 μg of each plasmid harboring PITX2, and EGFP, EmGFP, or TurboGFP as a fluorescent reporter, 2A or IRES2 sequences as a polycistronic sequence, and bovine

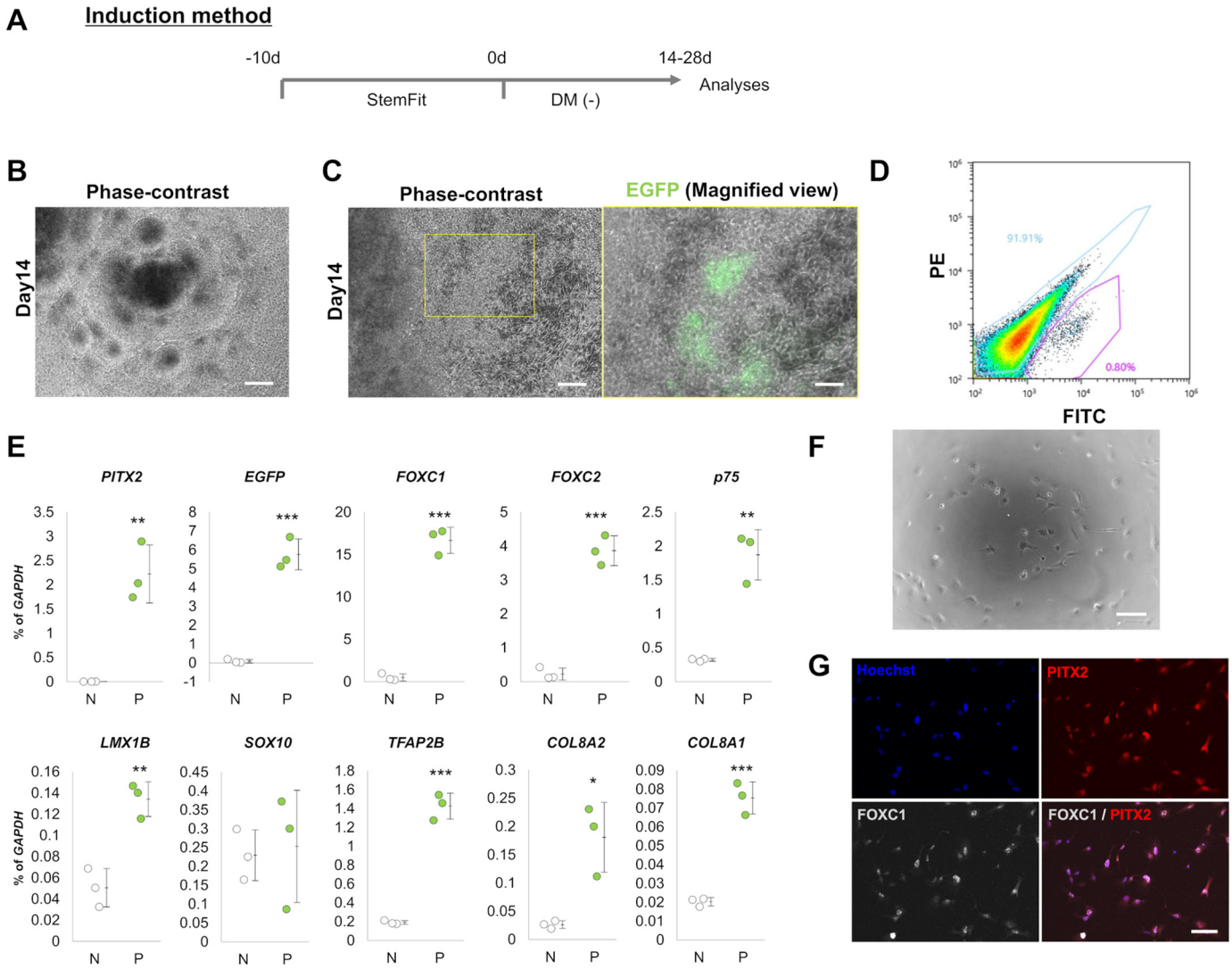

Figure 5. POM cells expressed in SEAMs in PITX2–EGFP knockin hiPSC clone 8-2 cells. *A*, schematic representation of the protocol used for SEAM induction. *B*, phase-contrast images of PITX2 knockin hiPSC clone 8-2. *Scale bar*, 200 μm. *C*, phase-contrast and fluorescence images of aggregated PITX2 knockin hiPSC clone 8-2 that express EGFP. *Scale bars*, 100 μm in the *left panel* and 50 μm in the *right panel*. *D*, FACS analysis of EGFP fluorescence intensity in 201B7 hiPSCs and PITX2 knockin hiPSC clone 8-2. The cells were expanded in PE (*y* axis) and FITC (*x* axis). The cells in the *blue polygon* are EGFP-negative, and those in the *purple polygon* are EGFP-positive. *E*, mRNA expressions of positive and negative markers of POM cell as determined by qRT-PCR in EGFP-negative and -positive cells after cell sorting. Expression levels are presented as dot plots of each value and the means ± standard deviation ($n = 3$). *, $p < 0.05$; **, $p < 0.01$; ***, $p < 0.001$. *N*, negative cells; *P*, positive cells. *F*, phase-contrast image of POM cells after 2 days of culture. *G*, immunofluorescence images of nuclei (*blue*), PITX2 (*red*), and FOXC1 (*gray*) in POM cells after 2 days of culture.

growth hormone, herpes simplex virus-thymidine kinase, SV40, PITX2 3′-UTR, and β-actin 3′-UTR as a polyadenylation signal were used in the experiments. After 24 h, fluorescence was evaluated and imaged using the Axio Observer D1. The experiments regarding recombinant DNA and genome-editing were approved by the research ethics committee of Osaka University and were performed in accordance with guidelines of Osaka University.

hiPSC culture

The hiPSC line 201B7 was kindly provided by the Center for iPS Cell Research and Application, Kyoto University (Kyoto, Japan). The cells were cultured on dishes seeded with MEFs in Dulbecco's modified Eagle's medium/F-12 (Thermo Fisher Scientific) supplemented with 20% knockout serum replacement (Thermo Fisher Scientific), 0.1 mM nonessential amino acids (Thermo Fisher Scientific), 0.1 mM 2-mercaptoethanol (Thermo Fisher Scientific), and 4 ng/ml bFGF (Fujifilm Wako Pure Chemical Corporation, Tokyo, Japan), with or without 10 μM Y-27632 (Fujifilm Wako Pure Chemical Corporation), which is selective inhibitor of Rho-associated coiled coil-forming protein kinases, to avoid apoptosis induction by electroporation. For feeder-free culture, the cells were cultured on dishes coated with iMatrix-511 (0.5 μg/cm^2; Nippi, Tokyo, Japan) in StemFit medium (Ajinomoto, Tokyo, Japan).

Construction of TALEN plasmids and the donor vector

PITX2 TALEN-L/R sequences were synthesized using GeneART Precision TALs (Thermo Fisher Scientific). Basic structure of the donor vector harboring an IRES2 (2A)-EGFP-SV40 poly(A)-neomycin cassette flanked by PITX2 homology arms was constructed by FASMAC (Kanagawa, Japan).

Establishment of the PITX2–IRES2–EGFP knockin hiPSC line

TALEN plasmids (2.5 μg) and donor vector (5 μg) were mixed in the solution included in the P3 primary cell 4D-Nucleofector™ X kit (Lonza, Basel, Switzerland) and were electroporated into 1.5×10^6 hiPSCs using program CB150 in the 4D-Nucleofector™ system (Lonza). The electroporated cells were seeded on DR4 MEFs (ASF-1001; Applied StemCell, Milpitas, CA) and were cultured for 5 days for recovery. The cells were cultured in the presence of G418 sulfate for 8 days and then in the absence of G418 sulfate for 4 days. Then the cells were picked up and transferred to a 12-well plate and cultured for 11 days. The cells were used for the screening of knockin colonies by end point PCR. Then the candidate knockin clone 8 was reseeded and screened as described above. The candidate knockin clone 8-2 was transferred to a 10-cm dish. Eventually, we used the heterozygous knockin clone 8-2, whose knockin sequence was confirmed by sequencing on an Applied Biosystems 3100 Genetic Analyzer (Thermo Fisher Scientific).

End point PCR for the screening of knockin colonies

Candidate clones were picked up and cultured in single wells of a 96-well plate. After 1 day, floating cells were harvested and lysed. The genomic DNA was extracted with a NucleoSpin tissue kit (Macherey-Nagel, Düren, Germany) and was used for end point PCR using Tks Gflex™ DNA polymerase (Takara Bio, Shiga, Japan) and two primer pairs. The primers were as follows: primer pair 1: forward: TGCATTCTAGTTGTGGTTTGTCC: reverse: AGTTTCTCTGGTGGATGCAATGA, thermal cycles: 94 °C for 1 min and 30 cycles of 98 °C for 10 s, 60 °C for 15 s, 68 °C for 30 s; primer pair 2: forward: TAGTAATCTGCACTGTGGCATCT, reverse: AGTTTCTCTGGTGGATGCAATGA, thermal cycles: 94 °C for 1 min and 30 cycles of 98 °C for 10 s, 60 °C for 15 s, 68 °C for 2 min.

Sanger sequencing

The cells were harvested and genomic DNA was extracted using a NucleoSpin® tissue kit (Macherey-Nagel). Sanger sequencing was conducted using Applied Biosystems 3730 DNA Analyzer and a BigDye™ Terminator version 3.1 cycle sequencing kit (both from Thermo Fisher Scientific), according to the manufacturer's instruction.

ALP staining

ALP staining was conducted using a TRACP and ALP double-stain kit (Takara Bio). Briefly, the cells were washed with PBS, fixed with fixation solution, and washed with water. The cells were treated with ALP substrate solution at 37 °C for 15 min and then washed twice with water. The cells were photographed using an EVOS FL auto imaging system (Thermo Fisher Scientific).

Immunofluorescence staining

hiPSC colonies, SEAMs, and POM cells were fixed with 4% paraformaldehyde and permeabilized with solution including 1% normal donkey serum, 0.3% Triton X-100 in TBS at 4 °C for 3 days or overnight. The colonies were treated with blocking solution (5% normal donkey serum, 0.3% Triton X-100 in TBS) for 1 h and then with primary antibodies against NANOG (Ab62734; Abcam), OCT3/4 (Ab19857; Abcam), SSEA-4 (MC-81370; BioLegend, San Diego, CA), and TRA-1–60 (330614; BioLegend) for 3 days. SEAMs were treated with primary antibodies against PAX6 (PRB-278P; BioLegend), p63 (sc-8431; Santa Cruz Biotechnology), α-crystallin (SPA-224; Stressgen Biotechnologies, San Diego, CA), CHX10 (sc-21690; Santa Cruz Biotechnology), and MITF (X1405M; Exalpha Biologicals, Shirley, MA) overnight. The POM cells were treated with primary antibody against PITX2 (Ab55599; Abcam) and FOXC1 (8758S; Cell Signaling Technology). Subsequently, the colonies and POM cells were labeled with secondary antibodies conjugated to Alexa Fluor 568, 594, 647, Plus 594, or Plus 647 (Thermo Fisher Scientific) for 1 h, counterstained with Hoechst 33342 (Thermo Fisher Scientific), and fluorescence images were acquired using an Axio Observer D1 or FLUOVIEW FV3000 (Olympus, Tokyo, Japan).

SEAM induction in hiPSCs

SEAMs were induced as described in our previous reports (22, 23). Briefly, hiPSCs were seeded in a 6-well plate coated with iMatrix-511 at 1500–4500 cells/well and cultivated in StemFit medium, with a medium change every 2–3 days. After 10 days, the medium was replaced with DM (Glasgow's minimum essential medium; Thermo Fisher Scientific) supplemented with 10% knockout serum replacement, 1 mM sodium pyruvate (Thermo Fisher Scientific), 0.1 mM nonessential amino acids (Thermo Fisher Scientific), 2 mM L-glutamine (Thermo Fisher Scientific), 1% penicillin–streptomycin solution (Thermo Fisher Scientific), and 55 μM 2-mercaptoethanol (Thermo Fisher Scientific) or monothioglycerol (Fujifilm Wako Pure Chemical Corporation), and the cells were cultivated for 4 weeks, with a medium change every 2–3 days. Then the medium was replaced with corneal DM consisting of DM and Cnt-20 or Cnt-PR without EGF and FGF2 (CELLnTEC Advanced Cell Systems, Bern, Switzerland) at 1:1, plus 20 ng/ml KGF (Fujifilm Wako Pure Chemical Corporation), 10 μM Y-27632, and 1% penicillin–streptomycin. For immunofluorescence staining of α-crystallin, CHX10, and MITF, the medium was directly replaced with corneal epithelium maintenance medium (Dulbecco's modified Eagle's medium/F-12 (2:1), Thermo Fisher Scientific) containing 2% B27 supplement (Thermo Fisher Scientific), 1% penicillin–streptomycin solution, 20 ng/ml KGF (Fujifilm Wako Pure Chemical Corporation), and 10 μM Y-27632 instead of corneal DM. The cells were cultivated for 4 weeks with a medium change every 2–3 days.

Induction of PITX2

Cranial neural crest and neural crest cells were induced from hPSCs as previously described (28–31). Using these cells as a reference, we established a POM cell induction method. hiPSCs were seeded in a 6-well plate coated with iMatrix-511 (0.5 μg/cm^2) at 1300–1500 cells/well. After 8 days of cultivation in StemFit medium, the medium was replaced with DM to start induction, and the cells were cultured for 2 days. Then the medium was replaced with DM containing 0–10 ng/ml BMP4 (R&D Systems, Minneapolis, MN) and 0–10 μM CHIR99021

(Sigma–Aldrich), and the cells were cultured for 2 days. Then the medium was replaced with DM without any additional reagents, and the cells were cultured for 4 days. Then the medium was replaced with DM containing 20 ng/ml EGF (R&D Systems) and 10 ng/ml bFGF, and the cells were cultured until analysis.

Western blotting analysis

The cells were lysed with radioimmune precipitation assay lysis and extraction buffer (Thermo Fisher Scientific) containing protease inhibitor mixture set I (Fujifilm Wako Pure Chemical Corporation) and sonicated. Protein concentrations were measured with a BCA protein assay kit (Thermo Fisher Scientific). The samples were analyzed using the WES system (ProteinSimple, San Jose, CA). Antibodies against GAPDH (sc-32233; Santa Cruz Biotechnology), PITX2 (Ab55599; Abcam), and GFP (sc-8334; Santa Cruz Biotechnology) were used. Other reagents, including secondary antibodies, were used following the manufacturer's instructions.

Flow cytometry

hiPSCs were cultured for 20 days and then dissociated with Accutase for 30 min. Accutase was removed by centrifugation, and the cells were resuspended in PBS. The cells were analyzed and sorted using an SH800 cell sorter (Sony, Tokyo, Japan). Aggregated cells were gated and excluded. Single cells were expanded in R-phycoerythrin (PE) and FITC to exclude autofluorescent cells. The cells were selected using polygon gates; the cells in the *purple polygon* were counted as EGFP-positive cells, whereas cells in the *blue polygon* were considered EGFP-negative cells.

qRT-PCR

Total RNA was extracted from cells that were manually harvested from each SEAM zones and from EGFP-negative and -positive cells sorted by flow cytometry, using QIAzol reagent (Qiagen). The RNA was reverse-transcribed into cDNA using the SuperScript III first-strand synthesis system for qRT-PCR (Thermo Fisher Scientific). qRT-PCRs were run using TaqMan Fast Universal PCR Master Mix (Thermo Fisher Scientific) and TaqMan minor groove binder probes against *GAPDH* (Hs99999905_m1), *TUBB3* (Hs00801390_s1), *SOX10* (Hs00366918_m1), RAX (Hs00429459_m1), *PAX6* (Hs00240871_m1), *DN-p63* (Hs00978339_m1), CDH1 (Hs01023894_m1), *KRT18* (Hs01941416_g1), *CRYAA* (Hs00166138_m1), *PITX2* (Hs00165626_m1), *EGFP* (Mr04329676_mr), *FOXC1* (Hs00559473_s1), *FOXC2* (Hs00270951_s1), *p75* (Hs00182120_s1), *LMX1B* (Hs00158750_m1), *TFAP2B* (Hs00231468_m1), *COL8A2* (Hs00697025_m1), and *COL8A1* (Hs00156669_m1) on an ABI Prism 7500 fast sequence detection system (Thermo Fisher Scientific). Thermal cycles were as follows: 95 °C for 20 s, 45 cycles of 95 °C for 3 s, and 60 °C for 30 s. Gene expression was normalized using *GAPDH* as an internal control.

Cultivation of EGFP-positive cells

EGFP-positive cells were sorted by FACS. The cells were attached to a plate coated with 0.5 μg/cm^2 iMatrix-511 and 1.56 μg/cm^2 fibronectin by centrifugation at 210 $\times$ *g* for 4 min. The cells were cultivated in DM with 10 μM Y-27632, 20 ng/ml EGF, 10 ng/ml bFGF, and 50–100 nM retinoic acid. After 2 days of cultivation, phase contrast images of the cells were captured using the Axio Observer D1.

Author contributions—T. O., R. H., Y. Kudo, Y. I., S. I., Y. Kobayashi, and A. H. resources; T. O. data curation; T. O., R. H., and S. K. formal analysis; T. O. and Y. Kudo validation; T. O., Y. Kudo, and Y. I. investigation; T. O. visualization; T. O., Y. Kudo, Y. I., S. I., Y. Kobayashi, and A. H. methodology; T. O. writing-original draft; R. H., S. K., and K. N. conceptualization; R. H., Y. H., S. K., and K. N. supervision; R. H., Y. H., S. K., and K. N. project administration; R. H., S. S., Y. I., and Y. Kobayashi writing-review and editing; K. N. funding acquisition.

Acknowledgments—We thank S. Hara for stimulating discussion and kind advice and E. Kimura and T. Katayama for providing technical support.

References

1. Mayor, R., and Theveneau, E. (2013) The neural crest. *Development* **140,** 2247–2251 CrossRef Medline
2. Beebe, D. C., and Coats, J. M. (2000) The lens organizes the anterior segment: specification of neural crest cell differentiation in the avian eye. *Dev. Biol.* **220,** 424–431 CrossRef Medline
3. Williams, A. L., and Bohnsack, B. L. (2015) Neural crest derivatives in ocular development: discerning the eye of the storm. *Birth Defects Res. C Embryo Today* **105,** 87–95 CrossRef Medline
4. Cvekl, A., and Tamm, E. R. (2004) Anterior eye development and ocular mesenchyme: new insights from mouse models and human diseases. *Bioessays* **26,** 374–386 CrossRef Medline
5. Langenberg, T., Kahana, A., Wszalek, J. A., and Halloran, M. C. (2008) The eye organizes neural crest cell migration. *Dev. Dyn.* **237,** 1645–1652 CrossRef Medline
6. Shiratori, H., Yashiro, K., Shen, M. M., and Hamada, H. (2006) Conserved regulation and role of Pitx2 in situs-specific morphogenesis of visceral organs. *Development* **133,** 3015–3025 CrossRef Medline
7. Lin, C. R., Kioussi, C., O'Connell, S., Briata, P., Szeto, D., Liu, F., Izpisúa-Belmonte, J. C., and Rosenfeld, M. G. (1999) Pitx2 regulates lung asymmetry, cardiac positioning and pituitary and tooth morphogenesis. *Nature* **401,** 279–282 CrossRef Medline
8. Campione, M., Steinbeisser, H., Schweickert, A., Deissler, K., van Bebber, F., Lowe, L. A., Nowotschin, S., Viebahn, C., Haffter, P., Kuehn, M. R., and Blum, M. (1999) The homeobox gene Pitx2: mediator of asymmetric left–right signaling in vertebrate heart and gut looping. *Development* **126,** 1225–1234 Medline
9. Franco, D., Sedmera, D., and Lozano-Velasco, E. (2017) Multiple roles of Pitx2 in cardiac development and disease. *J. Cardiovasc. Dev. Dis.* **4,** E16 Medline
10. Welsh, I. C., Thomsen, M., Gludish, D. W., Alfonso-Parra, C., Bai, Y., Martin, J. F., and Kurpios, N. A. (2013) Integration of left–right Pitx2 transcription and Wnt signaling drives asymmetric gut morphogenesis via Daam2. *Dev. Cell.* **26,** 629–644 CrossRef Medline
11. Suh, H., Gage, P. J., Drouin, J., and Camper, S. A. (2002) Pitx2 is required at multiple stages of pituitary organogenesis: pituitary primordium formation and cell specification. *Development* **129,** 329–337 Medline
12. Seo, S., Chen, L., Liu, W., Zhao, D., Schultz, K. M., Sasman, A., Liu, T., Zhang, H. F., Gage, P. J., and Kume, T. (2017) Foxc1 and foxc2 in the neural crest are required for ocular anterior segment development. *Invest. Ophthalmol. Vis. Sci.* **58,** 1368–1377 CrossRef Medline
13. McMahon, C., Gestri, G., Wilson, S. W., and Link, B. A. (2009) Lmx1b is essential for survival of periocular mesenchymal cells and influences Fgf-mediated retinal patterning in zebrafish. *Dev. Biol.* **332,** 287–298 CrossRef Medline

14. Evans, A. L., and Gage, P. J. (2005) Expression of the homeobox gene Pitx2 in neural crest is required for optic stalk and ocular anterior segment development. *Hum. Mol. Genet.* **14,** 3347–3359 CrossRef Medline
15. Chen, L., Martino, V., Dombkowski, A., Williams, T., West-Mays, J., and Gage, P. J. (2016) AP-2β is a downstream effector of PITX2 required to specify endothelium and establish angiogenic privilege during corneal development. *Invest. Ophthalmol. Vis. Sci.* **57,** 1072–1081 CrossRef Medline
16. Gage, P. J., Kuang, C., and Zacharias, A. L. (2014) The homeodomain transcription factor PITX2 is required for specifying correct cell fates and establishing angiogenic privilege in the developing cornea. *Dev. Dyn.* **243,** 1391–1400 CrossRef Medline
17. Kimura, M., Tokita, Y., Machida, J., Shibata, A., Tatematsu, T., Tsurusaki, Y., Miyake, N., Saitsu, H., Miyachi, H., Shimozato, K., Matsumoto, N., and Nakashima, M. (2014) A novel PITX2 mutation causing iris hypoplasia. *Hum. Genome Var.* **1,** 14005 CrossRef Medline
18. Gage, P. J., Rhoades, W., Prucka, S. K., and Hjalt, T. (2005) Fate maps of neural crest and mesoderm in the mammalian eye. *Invest. Ophthalmol. Vis. Sci.* **46,** 4200–4208 CrossRef Medline
19. Seifi, M., Footz, T., Taylor, S. A., Elhady, G. M., Abdalla, E. M., and Walter, M. A. (2016) Novel PITX2 gene mutations in patients with Axenfeld–Rieger syndrome. *Acta Ophthalmol.* **94,** e571–e579 CrossRef Medline
20. Tümer, Z., and Bach-Holm, D. (2009) Axenfeld–Rieger syndrome and spectrum of PITX2 and FOXC1 mutations. *Eur. J. Hum. Genet.* **17,** 1527–1539 CrossRef Medline
21. Lovatt, M., Yam, G. H., Peh, G. S., Colman, A., Dunn, N. R., and Mehta, J. S. (2018) Directed differentiation of periocular mesenchyme from human embryonic stem cells. *Differentiation* **99,** 62–69 CrossRef Medline
22. Hayashi, R., Ishikawa, Y., Sasamoto, Y., Katori, R., Nomura, N., Ichikawa, T., Araki, S., Soma, T., Kawasaki, S., Sekiguchi, K., Quantock, A. J., Tsujikawa, M., and Nishida, K. (2016) Co-ordinated ocular development from human iPS cells and recovery of corneal function. *Nature* **531,** 376–380 CrossRef Medline
23. Hayashi, R., Ishikawa, Y., Katori, R., Sasamoto, Y., Taniwaki, Y., Takayanagi, H., Tsujikawa, M., Sekiguchi, K., Quantock, A. J., and Nishida, K. (2017) Coordinated generation of multiple ocular-like cell lineages and fabrication of functional corneal epithelial cell sheets from human iPS cells. *Nat. Protoc.* **12,** 683–696 CrossRef Medline
24. Park, C.-Y., Kim, J., Kweon, J., Son, J. S., Lee, J. S., Yoo, J.-E., Cho, S.-R., Kim, J.-H., Kim, J.-S., and Kim, D.-W. (2014) Targeted inversion and reversion of the blood coagulation factor 8 gene in human iPS cells using TALENs. *Proc. Natl. Acad. Sci. U.S.A.* **111,** 9253–9258 CrossRef Medline
25. Fu, Y., Foden, J. A., Khayter, C., Maeder, M. L., Reyon, D., Joung, J. K., and Sander, J. D. (2013) High-frequency off-target mutagenesis induced by CRISPR-Cas nucleases in human cells. *Nat. Biotechnol.* **31,** 822–826 CrossRef Medline
26. Joung, J. K., and Sander, J. D. (2013) TALENs: a widely applicable technology for targeted genome editing. *Nat. Rev. Mol. Cell Biol.* **14,** 49–55 CrossRef Medline
27. Kobayashi, Y., Hayashi, R., Quantock, A. J., and Nishida, K. (2017) Generation of a TALEN-mediated, p63 knockin in human induced pluripotent stem cells. *Stem Cell Res.* **25,** 256–265 CrossRef Medline
28. Milet, C., and Monsoro-Burq, A. H. (2012) Neural crest induction at the neural plate border in vertebrates. *Dev. Biol.* **366,** 22–33 CrossRef Medline
29. Roy, O., Leclerc, V.B., Bourget, J.-M., Thériault, M., and Proulx, S. (2015) Understanding the process of corneal endothelial morphological change *in vitro*. *Invest. Ophthalmol. Vis. Sci.* **56,** 1228–1237 CrossRef Medline
30. Mimura, S., Suga, M., Okada, K., Kinehara, M., Nikawa, H., and Furue, M. K. (2016) Bone morphogenetic protein 4 promotes craniofacial neural crest induction from human pluripotent stem cells. *Int. J. Dev. Biol.* **60,** 21–28 CrossRef Medline
31. Fukuta, M., Nakai, Y., Kirino, K., Nakagawa, M., Sekiguchi, K., Nagata, S., Matsumoto, Y., Yamamoto, T., Umeda, K., Heike, T., Okumura, N., Koizumi, N., Sato, T., Nakahata, T., Saito, M., *et al.* (2014) Derivation of mesenchymal stromal cells from pluripotent stem cells through a neural crest lineage using small molecule compounds with defined media. *PLoS One* **9,** e112291 CrossRef Medline
32. Nishizawa, M., Chonabayashi, K., Nomura, M., Tanaka, A., Nakamura, M., Inagaki, A., Nishikawa, M., Takei, I., Oishi, A., Tanabe, K., Ohnuki, M., Yokota, H., Koyanagi-Aoi, M., Okita, K., Watanabe, A., *et al.* (2016) Epigenetic variation between human induced pluripotent stem cell lines is an indicator of differentiation capacity. *Cell Stem Cell* **19,** 341–354 CrossRef Medline
33. Hall, B. K. (2009) Pigment cells (chromatophores). In *The Neural Crest and Neural Crest Cells in Vertebrate Development and Evolution*, pp. 159–177, Springer, Boston, MA